



## One Pot Catalyzed Synthesis of 1,3-bis (2-(4-hydroxyphenyl)-2-methyl-4,5-diphenyloxazol-3(2H)-yl) Thiourea and Its Antimicrobial Activity

Vandana Singh\*, Jadveer Singh, Preeti, Arvind Kumar Pandey, Sneha Joshi, Lalit Mohan Dwivedi, Nauseen Fatima and Shailendra Tiwari

\*Department of Chemistry, University of Allahabad, **INDIA**

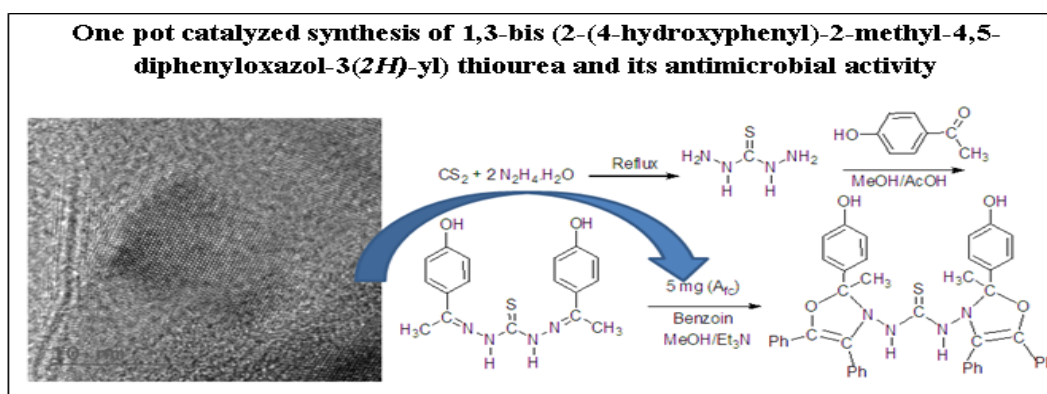
Email: [vschemau@gmail.com](mailto:vschemau@gmail.com)

Accepted on 19<sup>th</sup> September 2017, Published online on 27<sup>th</sup> September 2017

### ABSTRACT

*Aloevera-Fe<sup>0</sup>-Nps-Silica nanohybrid (A<sub>fc</sub>) catalyzed synthesis and antimicrobial activity of 1,3-bis (2-(4-hydroxyphenyl)-2-methyl-4,5-diphenyloxazol-3(2H)-yl) thiourea is being reported in the present communication. The catalyst was designed by integrating zerovalent FeNps (ZVI Nps) with Aloevera polysaccharide (AVP)-silica hybrid hydrogel. The synthesis of this new oxazole derivative (TO<sub>x</sub>) was performed in a single step using three components (thiocarbohydrazide, 4-hydroxy acetophenone, and benzoin) both through catalyzed and uncatalyzed routes. The catalyzed reaction led to 99.5 % product yield as compared to 49 % yield of the uncatalyzed reaction. The structure of TO<sub>x</sub> was established using C H N analysis, FTIR, and <sup>1</sup>H NMR spectroscopy. The catalyst was easily recycled for the synthesis. TO<sub>x</sub> exhibited fairly good antimicrobial activity against different strains of pathogenic bacteria and fungi. The minimum inhibitory concentration (MIC), minimum bactericidal concentration (MBC) and minimum fungicidal concentration (MFC) of TO<sub>x</sub> were determined using positive and negative controls.*

### Graphical Abstract



**Keywords:** Aloevera-Fe<sup>0</sup>-Nps-Silica nanohybrid, heterogeneous catalyst, oxazole nucleus, thiourea derivative, antimicrobial activity.

## INTRODUCTION

Gram-positive [1] and Gram negative pathogens [2] are responsible for a broad array of bacterial infections such as diarrhoea, rheumatic salmonellosis, leprosy, meningitis, pneumonia, food poisoning, extraintestinal, and intestinal wall infections. Antibiotics are unavoidable means for fighting these infections but the resistance of many pathogenic bacteria towards available antibiotics has emerged as the major threat to the human health [3]. Nevertheless fungal infections [4] are also of utmost concern as there is continuous increase in the number of immunocompromised hosts i.e. patients suffering from AIDS or those undergoing anticancer chemotherapy or organ transplantation. In this scenario, the development of new biologically active molecules is needed. One pot synthesis of drug-like small molecules is important as they are important scaffolds for drug discovery processes. The one pot routes provide these scaffolds in fewer steps [5]. The use of catalyst for such syntheses may further add advantage in terms of better yields and shorter reaction time [6]. The catalyzed route may be very productive in terms of product yield and selectivity. The oxazole nucleus are the key building blocks for many natural products, pharmaceuticals and the synthetic intermediates [7-9]. The oxazole ring plays a vital role in designing the active drugs that have analgesic, trypanocidal pro-apoptotic, antifungal, anti-inflammatory, antidepressant, pesticidal, and antimicrobial activities. Thiourea and its derivatives are known to exhibit a wide variety of biological activities such as antiviral, antibacterial, and antifungal. They find extensive applications in the field of medicine, agriculture and analytical chemistry. The union of heterocyclic ring with thiourea linkage often results compounds with enhanced biological performance [10]. AVP of Aloe vera gel consists of a backbone of  $\beta$ -(1 $\rightarrow$ 4)-D-mannosyl residues acetylated at C-2 and C-3 positions. It has 1:1 mannose monomer to acetyl ratio, while the backbone contains some side chains of mainly galactose that are attached to C-6 of the mannose units. The acemannan of Aloe vera is likely to template exciting new silica hybrid as it is structurally unique amongst the plant mannans [11]. The catalyzing role of iron [12] and iron nanoparticles [13,14] is known for many organic transformations. Iron is good catalytic substitute of noble metal catalysts because of its low cost and ubiquitous nature. Iron salts are known for catalyzing [15] the synthesis of few heterocyclic nuclei but the use of zerovalent iron nanoparticles ( $\text{Fe}^0\text{Nps}$ ) is yet not reported in literature. In principle,  $\text{Fe}^0\text{Nps}$  can offer great deal in terms of product yield and selectivity because of their large surface to volume ratio. The spent nanocatalysts can be easily separated and recycled since they exhibit better retention of catalytic activity than their bulk counterparts [16]. The synthesis of stable small sized  $\text{Fe}^0\text{Nps}$  involves tedious and sophisticated steps [17] as the small sized nanoparticles have a tendency to agglomerate in water under neutral condition to form micron scale or larger aggregates and they also have a tendency for slow corrosion [18]. Nanoparticles are either capped [19,20] or immobilized [21] in a polymer network structure to circumvent the problem of agglomeration. The impregnating nanoparticles with in polysaccharide templated silica matrix has emerged as a very useful technique for obtaining temperature resistant, stable and recyclable heterogeneous nanocatalysts [22,23]. In this light we have designed a novel catalyst from AVP, ZVI Nps and silica. The same has been utilized for synthesizing a new oxazole derivative; 1,3-bis (2-(4-hydroxyphenyl)-2-methyl, 4,5-diphenyl oxazol-3(2H-yl) thiourea ( $\text{TO}_x$ ) in a one pot method.  $\text{TO}_x$  has been screened for its antimicrobial activity. The synthesis of the target compound was planned due to reported biological activity of thiourea coupled oxazole moieties [24,25]. This catalyst invite sustainable approach for using polysaccharides derived nanocatalysts for synthesizing heterocyclic systems.

## MATERIALS AND METHODS

**Chemicals and instrumentation:** TERRA-PURE™, USA certified spray dried aloe vera inner leaf powder regular, 200 x (Specific gravity- 0.997- 1.004) was used after reprecipitation in ethanol. Tetramethoxysilane (TMOS), iron(III) nitrate nanohydrate, methanol, acetic acid (MERCK, India) were used. Methanol extra pure (LOBA Chemie) was used. Mango leaves were locally collected from Allahabad University campus and were powdered after drying in shade.  $\text{CS}_2$ , hydrazine, 4-hydroxy acetophenone, Benzoin (Aldrich, USA) were used. UV/Vis Spectrophotometer UV 100 (Cyber lab, USA)

was used to observe the surface plasmon of zerovalent FeNps (ZVI Nps). All the melting points that were measured with a capillary apparatus are uncorrected. TEM analysis was done on FEI Technai U- Twin 20 instrument. HRTEM, EDX and elemental mapping was conducted using a FEI Titan G2 60-300 TEM (HR-TEM) instrument. X-ray diffraction (Cu K $\alpha$  source) of the powdered sample was carried out on a XRD Pananalytical X-Pert Pro X-ray powder diffractometer. Elemental analysis was done on Haraeus Carbo Erba 1108 elemental analyzer. IR spectra were recorded using KBr pellets on a Perkin-Elmer model 400 FTIR spectrometer.  $^1\text{H}$  NMR spectra were recorded at ambient temperature using a 500 MHz (ZEOL-500) NMR spectrometer in DMSO- $d_6$ . All the experiments were performed in triplicate and the results reported are the average of three experiments. The bacterial and fungal stock cultures were incubated for 24 hours at 37°C on nutrient agar and potato dextrose agar (PDA) medium, respectively, following refrigeration storage at 4°C. The bacterial strains were grown in Mueller-Hinton agar (MHA) plates at 37°C (the bacteria were grown in the nutrient broth at 37°C and maintained on nutrient agar slants at 4°C). The fungal strains were grown in Sabouraud dextrose agar and PDA media, respectively at 28°C. The stock cultures were maintained at 4°C.

**Purification of Aloe vera polysaccharide:** A homogenous solution was obtained by stirring aloe vera powder (2 g) in distilled water (25 mL) for 15-20 min. This solution was precipitated with ethyl alcohol (200 mL) to obtain the aloe vera polysaccharide. The polysaccharide was dried and reprecipitated thrice to obtain the pure polysaccharide (AVP) that was dried and used for the catalyst synthesis.

**Synthesis of ZVI Nps:** ZVI Nps were prepared using mango leaf extract. Mango leaf extract was prepared by boiling 1.0 g dried mango leaf powder with 25 mL of distilled water till the volume was reduced to 10 mL. The typical procedure for preparing ZVI Nps is described below:

Mango leaf extract (5 mL) was added to ferric nitrate solution (5 mL of 0.1 M) whereupon the yellow ferric nitrate solution immediately turned black due to the formation of ZVI Nps. The formation of ZVI Nps was confirmed by observing surface plasmon peak for ZVI Nps [26].

**Synthesis of catalyst:** The hybrid catalyst was synthesized by using sol gel approach for which 0.2 g AVP was dissolved in 7 mL distilled water. To this solution 1.0 mL TMOS and 1.0 mL MeOH were added. ZVI Nps solution (3 mL) was added to this mixture after 10 min of stirring on a magnetic stirrer at room temperature and the mixture was stirred till the hydrogel was formed (180 min). It was dried overnight in an electric oven at 45 °C and powdered well before use.

**Recycling of catalyst:** The catalyst (10 mg) was stirred with 5 mL distilled water at 100 rpm on a magnetic stirrer, filtered, dried and was reused in the requisite amount (0.005 g) for the synthesis of TOx as described below.

#### Synthesis of oxazole derivative

**Synthesis of thiocarbonohydrazide:** Thiocarbonohydrazide was synthesized by a known method where carbon disulphide was directly added to excess of hydrazine hydrate (3 M) at its boiling point. Thiocarbonohydrazide was periodically removed (60 % yield). The crude product was recrystallized with water (m.p. 168 °C).

**Synthesis of 1,3-bis (2-(4-hydroxyphenyl)-2-methyl-4,5-diphenyloxazol-3(2H)-yl) thiourea:** Thiocarbonohydrazide (1.06 g, 0.01M), 4-hydroxy acetophenone (2.72 g, 0.02M), and benzoin (4.24 g, 0.02M) were dissolved in 30 mL of methanol. To this solution 0.005 g of catalyst and two drops of triethyl amine were added and the mixture was refluxed for 2 h. It was filtered hot to remove the catalyst. The excess solvent was removed in a rotary evaporator and the reaction mixture was poured over crushed ice. The solid mass thus obtained was filtered and recrystallized from aq. ethanol and dried (yield 7.5 g).

The identical reaction was performed in absence of  $A_{fc}$ . The product formation was monitored by TLC (solvent: ethylacetate). The product yields were determined for both the catalyzed and uncatalyzed reaction. The identities of the products obtained through the catalyzed and uncatalyzed procedure were determined by their melting points, FTIR,  $^1\text{H}$  NMR and TLC. The solubility of the products in various organic solvents was also determined.

## RESULTS AND DISCUSSION

**Characterization of catalyst ( $A_{fc}$ ):** In FTIR spectrum (Fig. 1), the aloe vera O-H and silica silanols are together seen as merged peak at  $3444\text{ cm}^{-1}$ . Carbonyl stretching peaks of O-acetyl ester is seen at  $1734\text{ cm}^{-1}$  while other C-O stretching peak is seen masked with silica peaks below  $1250\text{ cm}^{-1}$ . -C-CH<sub>3</sub> bending absorption is present at  $1384\text{ cm}^{-1}$ . Peaks due to SiO-H, Si-OH, and O-Si-O stretching are observed at  $3398\text{ cm}^{-1}$  (merged with O-H peak),  $1083\text{ cm}^{-1}$  and  $798\text{ cm}^{-1}$  respectively.

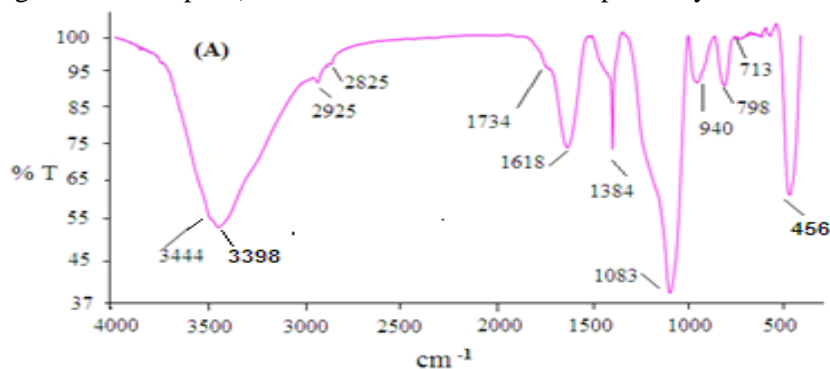


Fig. 1: FTIR spectra  $A_{fc}$

FE-SEM imaging of the catalyst ( $A_{fc}$ ) (Fig. 2(A&B)), exhibited layered hybrid surface enveloped with nearly spherical to spherical shaped ZVI nanoparticles that are slightly agglomerated at places.

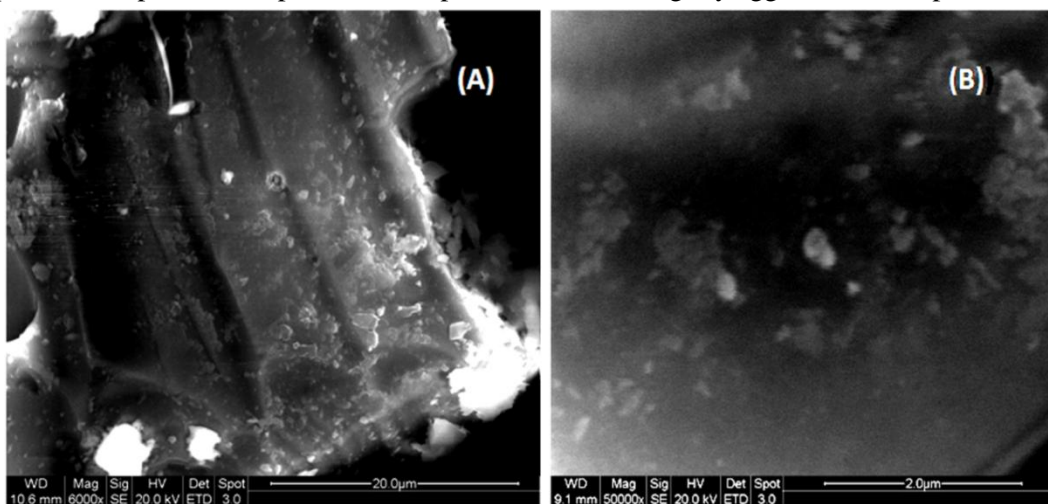
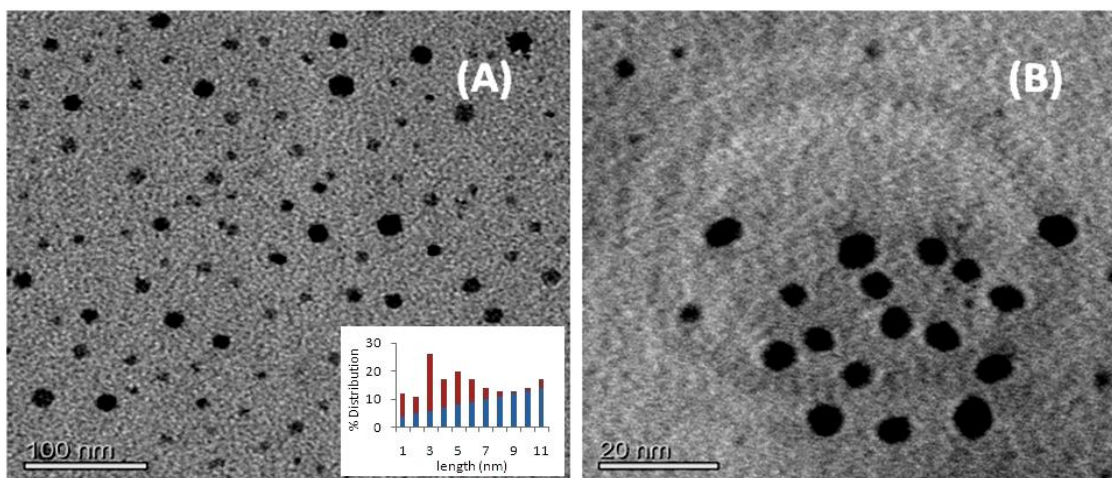


Fig. 2: (a) FE-SEM imaging of the  $A_{fc}$  (A) 6000X and (B) 50000X

TEM picture of  $A_{fc}$  (catalyst) is depicted in Fig. 3, where particles are spherical to nearly spherical but slightly agglomerated ZVI Nps are seen scattered within the hybrid silica matrix. The TEM histogram prepared by IMAGE J software revealed that ZVI Nps are in the range of 1-11 nm, average particle size being  $\sim 5$  nm (Fig. 3(A)). The hybrid matrix is uniform and throughout decorated with the ZVI Nps.



**Fig. 3:** Transmission Electron Micrographs of  $A_{fc}$  at different magnification (A) and (B); TEM histogram seen as inset of (A).

High resolution TEM (HRTEM) revealed fringes of regular lines within nearly spherical FeNPs that are dispersed in silica matrix (Fig. 4(A&B)). The fine  $Fe^0$  crystallites have a diameter of  $\sim 5$  nm and its lattice fringes have the spacing of 0.282 nm which is in good agreement with the (110) plane of zerovalent iron nanoparticle [29]. HAADF image of  $A_{fc}$  depicted the chemical composition inside the nanocomposite at sub-nanometer resolution (Fig. 5(A-C)). The EDX mapping of elements in a selected area of  $A_{fc}$  (Fig. 4(D)), revealed the presence of Fe with other elements Si, C, O, N (constituent of mango leaf extract). This observation has confirmed the inclusion of ZVI in the composite. The SAED pattern indicate the polycrystalline nature of the catalyst matrix with embedded  $Fe^0$  Nps.

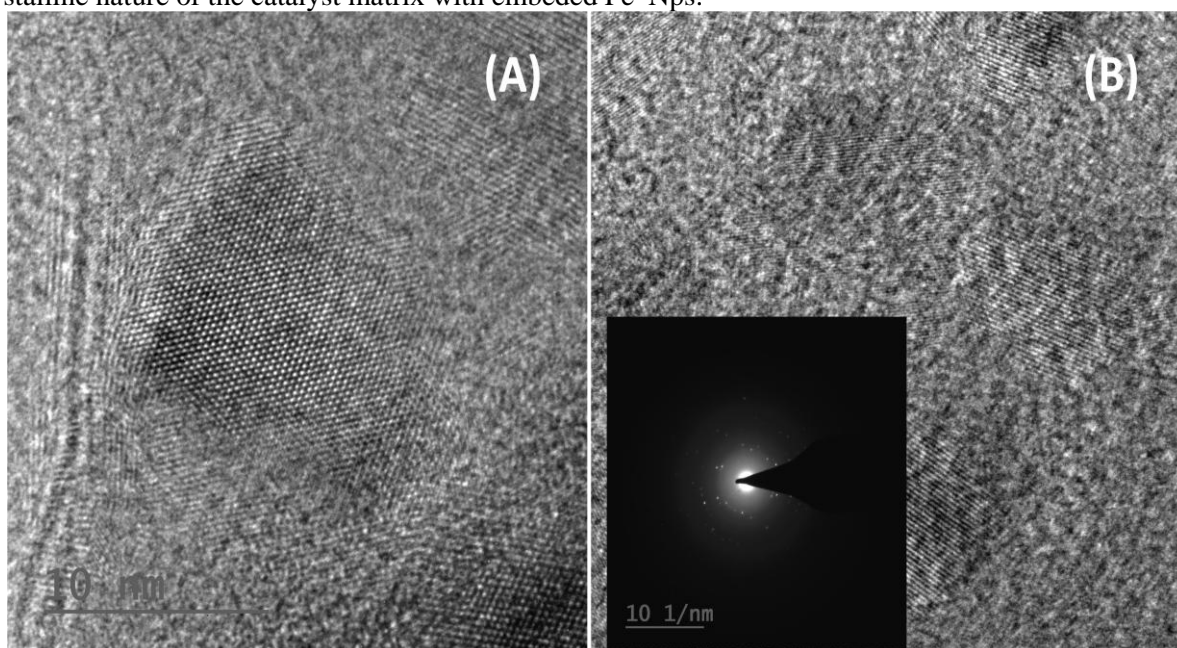


**Fig. 4:** High resolution TEM image (A) High Magnification of a single  $Fe(0)$  NP showing lattice fringes (B) HRTEM of  $A_{fc}$  with SAED pattern seen in inset

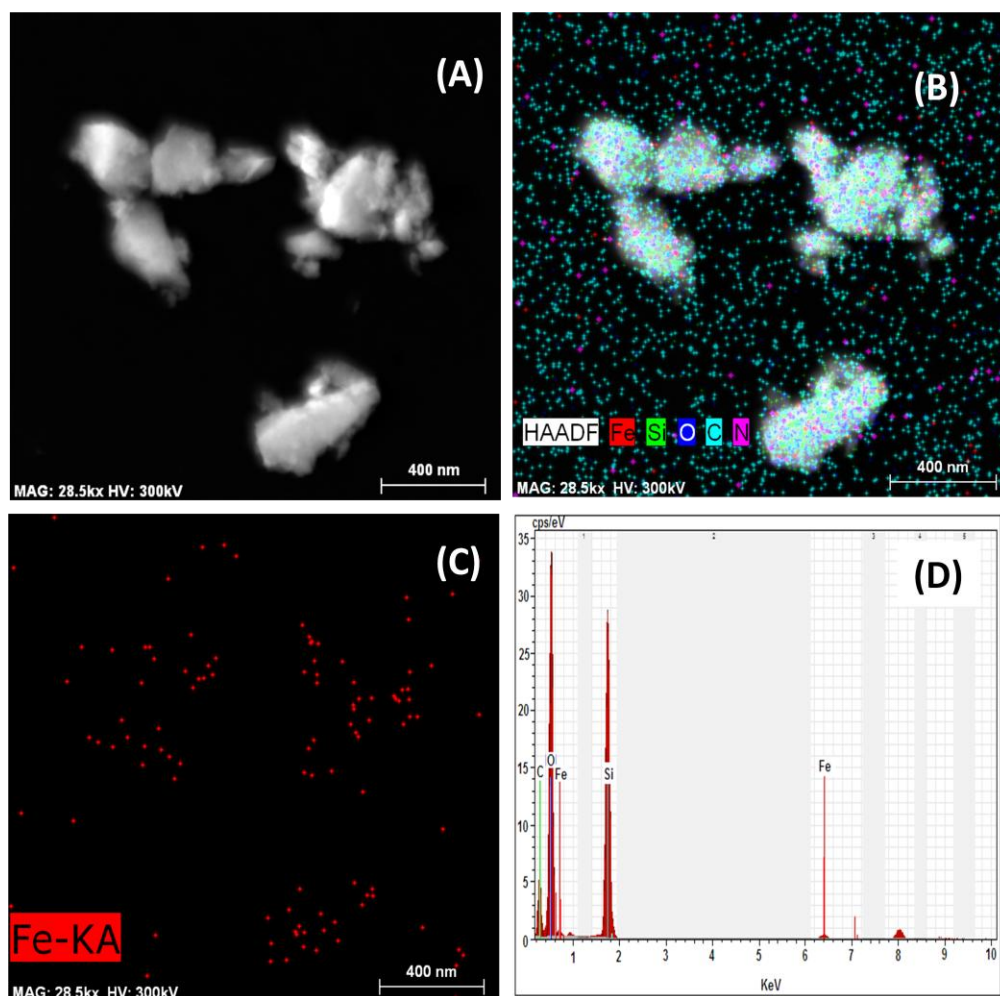


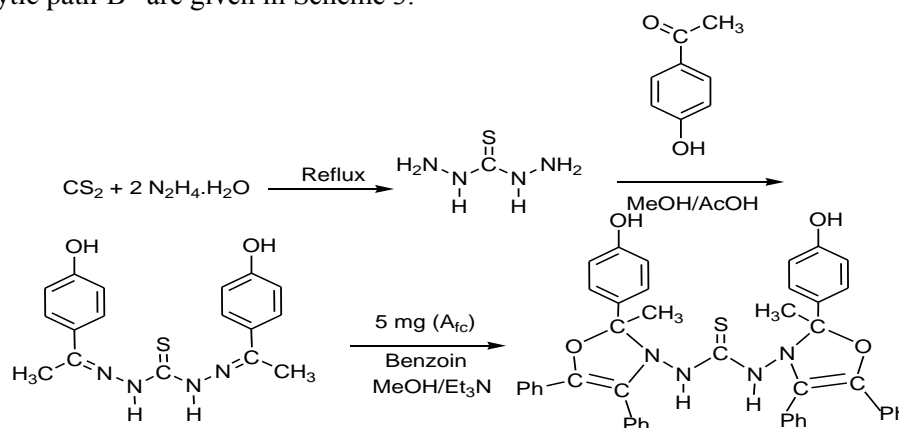
**Fig. 5:** (A&B) HAADF HR-TEM image of  $A_{fc}$  and its corresponding elemental mappings for (C) Fe, (D) The corresponding EDX spectrum taken from the whole area of (A).

**The catalytic activity of the  $A_{fc}$ :** The catalyst synthesis involved AVP templated polymerization of tetramethoxysilane in presence of ZVI Nps which were synthesized by reducing  $Fe^{+3}$  salt with aqueous extract of dry powdered mango leaf according to a previously known method [26]. The selection of  $H_2O$ : TMOS: MeOH ratio was based upon our previous experience [27] with similar materials derived from other polysaccharides. The catalyst was obtained using 0.2 g of purified [28] AVP, 1.0 mL TMOS, 1.0 mL MeOH, and 10 mL water (which included the water content in the Nps solution). The purpose of impregnation of ZVI Nps in AVP templated silica was to avoid agglomeration of nanoparticle during the catalyzed reaction of the oxazole nucleus and easy recovery of the catalyst for the recycling. The selection of AVP as the templating agent was based on its unique structural characteristics among the plant mannan polysaccharides. The catalyst ( $A_{fc}$ ) has polycrystalline nature having both AVP and silica matrix with embeded  $Fe^0$  Nps of ~5 nm diameter.

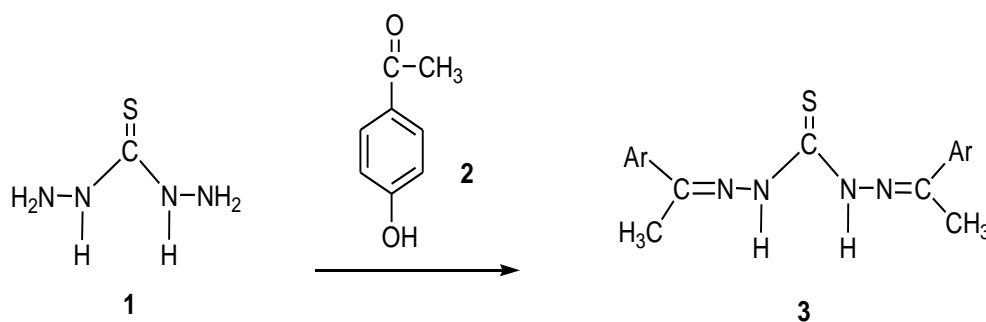
The catalytic activity of the  $A_{fc}$  has been monitored for one pot three component synthesis of 1,3-bis (2-(4-hydroxyphenyl)-2-methyl-4,5-diphenyloxazol-3(2*H*)-yl) thiourea (Scheme 1) for which thiocarbonyl hydrazide **1**, 4-hydroxy acetophenone **2** and benzoin **3** were taken in methanol and refluxed for 2 h along with catalyst ( $A_{fc}$ ) and triethyl amine. **1** was synthesized by a known method [30], where carbon disulphide was directly added to excess of hydrazine hydrate (3 M) at its boiling point. **1** was periodically removed (60 % yield). The crude product was recrystallized with water (m.p. 168 °C).

The reaction mixture was poured over crushed ice after removal of the catalyst. The solid mass thus obtained was filtered and recrystallized from aq. ethanol, yield 7.5 g (corresponding to 99.5 %), m.p 105 °C. A schematic diagram for the synthesis of the 1,3-bis (2-(4-hydroxyphenyl)-2-methyl-4,5-diphenyloxazol-3(2*H*)-yl) thiourea is depicted as Scheme 1. The same product was obtained for uncatalyzed reaction but now product yield was just 3.6 g (49 %) and the completion of the reaction required 4 h reflux time. The catalyst was recycled after through washing with water and in second cycle the product yield in the catalyzed reaction was 6.4 g (85%).

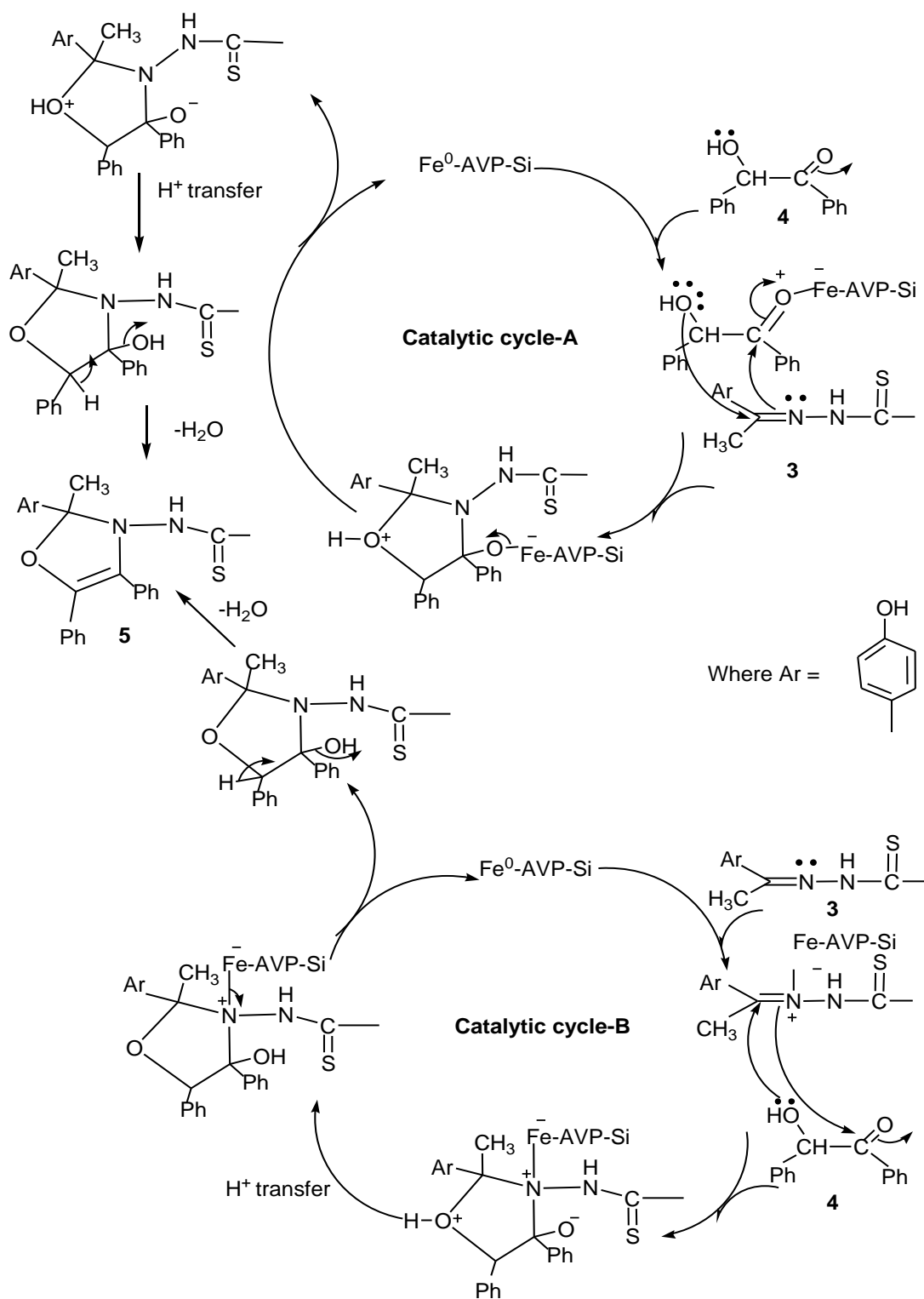
First step is the reaction of thiocarbonohydrazide **1** with 4-hydroxyacetophenone **2** to form corresponding Schiff's base **3** (Scheme 2). We speculate that the  $\text{Fe}^0$  of  $\text{A}_{\text{fc}}$  catalyst, having vacant d orbitals act as electrophile, thus induces more electrophilic character at carbonyl carbon atom of benzoin (Catalytic Path-A) **4** and/or at C-atom of azomethine (Catalytic Path-B) of **3** respectively. Thus attack of nucleophile in either case becomes easier. This is the reason that the addition of the catalyst in this reaction reduces reaction time period and increase the yield of the final product. Two possible mechanisms "Catalytic path-A" and "Catalytic path-B" are given in Scheme 3.



**Scheme 1.** Schematic diagram for the synthesis of 1,3-bis (2-(4-hydroxyphenyl)-2-methyl-4,5-diphenyloxazol-3(2*H*)-yl) thiourea



**Scheme 2.** Synthesis of thiocarbonohydrazide



**Scheme 3.** Plausible mechanistic pathways for the catalytic synthesis of 1,3-bis(2-(4-hydroxyphenyl)-2-methyl, 4,5-diphenyl oxazol-3(2H)-yl) thiourea



**Physical and Spectral data of synthesized 1,3-bis (2-(4-hydroxyphenyl)-2-methyl-4,5-diphenyloxazol-3(2H)-yl) thiourea (TO<sub>x</sub>):**

Solubility	DMF, DMSO, ethylacetate, acetone, ethanol; insoluble in benzene, toluene, hexane, cyclohexane, and chloroform
Melting point	105°C
R <sub>f</sub> (Solvent: ethylacetate)	0.44
IR (KBr)	3415 (O-H), 3375 (-NH), 3060, 2931 (C-H str.), 1689 (C=C str.), 1304 (C-N str.), 1304-1340 (C-H bending), 1261 (phenolic C-O phenolic str.), 1206 (C-O str.), 1068 (C-O str.), 1003 (N-N str.), 1200 (C=S str.), 1490 (CH <sub>3</sub> as), 1388 (CH <sub>3</sub> s), 704, (C-H bend mono subst. Ar), 754 (C-H bend di subst. Ar), 682-1003 (C-H bend Ar), 1600, 1490 and 1178 cm <sup>-1</sup> (C=C Ar.)
<sup>1</sup> H NMR (DMSO-d <sub>6</sub> ):	δ 6.87-7.95 (m, aromatic H), 1.19 (s, CH <sub>3</sub> ), 6.31 (O-H), 6.27 (N-H)
Elemental Analysis	Anal. Calcd for C <sub>47</sub> H <sub>42</sub> N <sub>4</sub> O <sub>4</sub> S; C, 73.90; H, 5.20; N, 7.67; Found C, 73.75; H, 5.25; N, 7.70.

**Biological activity of oxazole derivative (TO<sub>x</sub>):** The synthesized oxazole derivative (TO<sub>x</sub>) is a new compound and therefore we were prompted to screen its antibacterial and antifungal activities. Antibacterial activity of TO<sub>x</sub> was screened against *E. coli* (ATCC-25922), Methicillin-resistant *S. aureus* (MRSA +ve), *Pseudomonas aeruginosa* (ATCC-27853), *Streptococcus pyogenes* and *K. pneumonia* (Clinical isolate) bacterial strains by disk diffusion method [31]. The Minimum Inhibitory Concentration (MIC) are summarized in Table. 1 and Table. 2 respectively.

The investigation of antibacterial screening data revealed that TO<sub>x</sub> has fairly good bacterial inhibition against *S. Pyogenes*, Methicillin-resistant *S. aureus* (MRSA +ve), *P. Aeruginosa*, *K. Pneumonia*, and *E. coli* species. The compound showed antibacterial activity (MIC 12.5 µg mL<sup>-1</sup>) against all bacterial strains except for *E. Coli* for which MIC was 25 µg mL<sup>-1</sup>. The minimum bactericidal concentration (MBC) of the compound was two, three, or four fold higher than the corresponding MIC results.

**Table 1.** Antibacterial activity of the compound

Diameter of zone of inhibition (mm)					
Gram positive bacteria			Gram Negative bacteria		
Compounds	<i>S. pyogenes</i>	MRSA <sup>a</sup>	<i>P. aeruginosa</i>	<i>K.pneumonia</i>	<i>E. coli</i>
TO <sub>x</sub>	19.5±0.3	16.1±0.5	24.4±0.2	15.3±0.2	20.1±0.3
Standard	22.0±2.0	21.0±0.2	31.0±0.3	19.0±0.2	27.0±0.2
DMSO	--	---	---	---	---

Positive control (standard); Ciprofloxacin and negative control (DMSO) measured by the halo zone test (Unit, mm) a Methicillin resistant *S. aureus*(MRSA +ve)

**Table 2.** MIC and MBC results of TO<sub>x</sub> and positive control Ciprofloxacin

Diameter of zone of inhibition (mm)										
Gram positive bacteria				Gram Negative bacteria						
Compounds	<i>S. pyogenes</i>		MRSA <sup>a</sup>		<i>P. aeruginosa</i>		<i>K.pneumonia</i>		<i>E. coli</i>	
	MIC	MBC	MIC	MBC	MIC	MBC	MIC	MBC	MIC	MBC
TO <sub>x</sub>	12.5	25	12.5	25	12.5	25	12.5	50	25	50
Standard	12.5	12.5	6.25	12.5	12.5	25	6.25	25	6.25	12.5
DMSO	--	--	--	--	--	--	--	--	--	--

MIC(µg/mL) minimum inhibitory concentration, i.e the lowest concentration of the compound to inhibit the growth of bacteria completely.  
MBC(µg/mL) minimum bactericidal concentration, i.e the lowest concentration of compound for killing the bacteria completely

Antifungal activity was also studied using the disk diffusion method. For assaying antifungal activity, *C. albicans*, *Aspergillus fumigatus*, *Penicillin marneffi* and *Trichophyton mentagrophytes* were re-cultured in DMSO by agar diffusion method [32].

The inhibitory results are presented in Table. 3 and Table. 4. The antifungal screening data showed fairly good fungicidal activity against *C. albicans*, *Aspergillus fumigatus*, *Penicillin marneffi* and *Trichophyton mentagrophytes* fungal strains. The compound showed maximum inhibition results against *C. albicans*, and *T. Mentagrophytes*. The MFC of the compound was found to be two, three, or four fold higher than the corresponding MIC results.

**Table 4.** Antifungal activity of compounds TOx

Compounds	<i>C. albicans</i>	<i>A. fumigates</i>	<i>T. mentagrophytes</i>	<i>P. marneffi</i>
TOx	18.1±0.3	15.7±1.2	18.3±0.7	12.1±0.2
Standard	30.0±0.2	27.0±0.2	24.0±0.3	20.0±0.5
DMSO	--	---	---	---

Positive control (Griseofulvin) and negative control (DMSO) measured by the halo zone test (Unit, mm).

**Table 5.** MIC and MFC of TOx

Compounds	<i>C. albicans</i>		<i>A. fumigates</i>		<i>T. mentagrophytes</i>		<i>P. marneffi</i>	
	MIC	MFC	MIC	MFC	MIC	MFC	MIC	MFC
TOx	25	100	25	50	25	50	25	100
Standard	6.25	25	12.5	12.5	6.25	25	12.5	25

MIC ( $\mu\text{g mL}^{-1}$ ) minimum inhibitory concentration i.e the lowest concentration of the compound to inhibit the growth of fungus completely  
MFC ( $\mu\text{g mL}^{-1}$ ) minimum fungicidal concentration, i.e the lowest concentration of the compound for killing the fungus completely.

## APPLICATIONS

In the current study, Aloe vera-Fe<sup>0</sup>-Nps-Silica composite were found to be an efficient catalyst for the synthesis of 1,3-bis (2-(4-hydroxyphenyl)-2-methyl-4,5-diphenyloxazol-3(2H)-yl) thiourea (TO<sub>x</sub>). The synthesized new oxazole derivative (TO<sub>x</sub>) showed fairly good antibacterial and antifungal activity.

## CONCLUSIONS

In summary, an efficient, clean and convenient one-pot three components synthesis of a new oxazole derivative; 1,3-bis (2-(4-hydroxyphenyl)-2-methyl-4,5-diphenyloxazol-3(2H)-yl) thiourea was carried out through catalyzed and uncatalyzed routes. The catalyzed synthesis gave double yield (99 %) as compared to the uncatalyzed reaction (45 %). The catalyzed synthesis has an advantage of excellent yield and shorter reaction time and the catalyst was successfully used in the second cycle without compromising its activity. The catalyst (A<sub>fc</sub>) was designed from Aloe vera acetomannan which has ZVI Nps of ~5 nm size impregnated within aloe vera-silica hybrid matrix. The A<sub>fc</sub> showed fairly good antimicrobial activity. TO<sub>x</sub> can be used as template for synthesizing several derivatives through modification to develop bioactive heterocyclic oxazole compounds while the catalyst may be useful for synthesizing the similar other heterocyclic nuclei.

## ACKNOWLEDGEMENTS

The authors thank UGC, New Delhi for the financial support and I.I.T., Kanpur, India for FE Quanta SEM, HRTEM, <sup>1</sup>HNMR, CHN, and FTIR studies. XRD is acknowledged to Department of Mineralogy and Petrology, University of Allahabad, and elemental analysis is acknowledged to Central Drug Research Institute, Lucknow, India. The authors are thankful to the Head, Department of Chemistry, University of

Allahabad, Allahabad for providing necessary chemicals. Prof. S. Sundaram, Department of Biotechnology, University of Allahabad, Allahabad for evaluating biological activity.

## REFERENCES

- [1] E. Bouza, R. Finch, Infections caused by Gram – positive bacteria: situation and challenges of treatment, *Clin. Microbiol. Infect.*, **2001**, 7, 1-99.
- [2] A. Y. Peleg, D. C. Hooper, Hospital-Acquired Infections Due to Gram-Negative Bacteria, *N. Engl. J. Med.*, **2010**, 362, 1804–1813.
- [3] K. H. Luepke, K. J. Suda, H. Boucher, R. L. Russo, M. W. Bonney, T. D. Hunt, J. F. Mohr III, Past, Present, and Future of Antibacterial Economics: Increasing Bacterial Resistance, Limited Antibiotic Pipeline, and Societal Implications, *Pharmacotherapy*, **2017**, 37, 71-84.
- [4] K. Avasthi, R. Yadav, T. Khan, Greener and efficient synthesis of some novel substituted azitidinones with 4-amino pyridine via heterogenous catalyst, *J Applicable Chem*, **2014**, 3, 1899-1906
- [5] N. J. P. Subhashini, A. K. Pagudala, Ch.B. Reddy, B.Lingaiah, One Pot Synthesis and Characterization of 1,2,3-Triazole Xanthenones As Potent Anti-Bacterial Agents, *J Applicable Chem*, **2015**, 4, 1534-1540
- [6] J. D. Bhirud, H. P. Narkhede, Potassium dihydrogen phosphate: An inexpensive catalyst for the synthesis of 2, 4, 5- trisubstituted imidazoles under solvent free condition, *J Applicable Chem*, **2016**, 5, 1075-1079.
- [7] B. H. Norman, L.F. Lee, J. L. Masferrer, J. J. Talley, 2-substituted oxazoles further substituted by 4-fluorophenyl and 4-methylsulfonylphenyl as antiinflammatory agents, *US patent* 5380738 A, **1995**.
- [8] M. Kaspady, V.K. Narayanaswamy, M. Raju, G.K. Rao, Synthesis, Antibacterial Activity of 2,4-Disubstituted Oxazoles and Thiazoles as Bioisosteres, *Lett Drug Des Discov*, **2009**, 6, 21-28.
- [9] E. Mann and H. Kessler, New Oxazole-Based Peptidomimetics: Useful Building Blocks for the Synthesis of Orthogonally Protected Macrocyclic Scaffolds, *Org. Lett.*, **2003**, 5, 4567-4570.
- [10] S. Saeed, R. Hussain, A convenient way for the preparation of novel thiourea derivatives containing biologically active quinazoline moiety, *Eur Chem Bull*, **2013**, 2, 465-467.
- [11] J. H. Hamman, Composition and Applications of *Aloe vera* Leaf Gel, *Molecules*, **2008**, 13, 1599-1616.
- [12] J. Bonnamour, C. Bolm, Iron-Catalyzed Intramolecular *O*-Arylation: Synthesis of 2-Aryl Benzoxazoles, *Org. Lett.*, **2008**, 10, 2665–2667.
- [13] R. Hudson, G. Hamasaka, T. Osako, Y. M. A. Yamada, C-J. Li, Y. Uozumi, A. Moores, Highly efficient iron(0) nanoparticle-catalyzed hydrogenation in water in flow, *Green Chem.*, **2013**, 15, 2141-2148.
- [14] C. Rangheard, C. de Julián Fernández, P. H. Phua, J. Hoorn, L. Lefort, J. G. De Vries, At the frontier between heterogeneous and homogeneous catalysis: hydrogenation of olefins and alkynes with soluble iron nanoparticles, *Dalton Trans.*, **2010**, 39, 8464–8471.
- [15] M. Wu, X. Hu, J. Liu, Y. Liao, G.-J. Deng, Iron-Catalyzed 2-Arylbenzoxazole Formation from *O*-Nitrophenols and Benzylic Alcohols, *Org. Lett.*, **2012**, 14, 2722–2725.
- [16] G. Fischer, R. Poteau, S. Lachaize, I. C. Gerber, Surfaces of a Colloidal Iron Nanoparticle in Its Chemical Environment: A DFT Description, *Langmuir*, **2014**, 30, 11670–11680.
- [17] L. Parimala, J. Santhanalakshmi, Studies on the Iron Nanoparticles Catalyzed Reduction of Substituted Aromatic Ketones to Alcohols, *J of Nanopart.*, **2014**, 2014, 1-10.
- [18] D. Li, J. Zhu, J. Wu, W. Yin, H. Liang, G. G. Lin, Development of an activated carbon-supported zero-valent iron catalyst (AC-Fe<sup>0</sup>) for enhancing degradation of reactive brilliant orange and reducing iron sludge production, *Environ Prog Sustain Energy.*, **2016**, 35, 949-956.
- [19] C. Gutiérrez-Wing, J. J. Velázquez-Salazar, M. José-Yacamán, Procedures for the Synthesis and Capping of Metal Nanoparticles, *Methods Mol Biol.*, **2012**, 906, 3-19.

- [20] S. Dhupar, D. Panda, P. L. Nayak, Green Synthesis and Characterization of Zero Valent Iron Nanoparticles from the Leaf Extract of *Mangifera indica*, *Nanotrends, A Journal of Nanotechnol and its Application*, **2012**, 13, 16-22.
- [21] Q. Zhu, Q. Pan, Mussel-Inspired Direct Immobilization of Nanoparticles and Application for Oil-Water Separation, *ACS Nano*, **2014**, 8, 1402-1409.
- [22] H.E. Emam, B. A. Hanan, Polysaccharides templates for assembly of nanosilver, *Carbohydr Polym.*, **2016**, 135, 300-307.
- [23] V. Singh, A. K. Pandey, P. Srivastava, J. Singh, T. Malviya, Gum acacia-CuNp-silica hybrid: an effective, stable and recyclable catalyst for reduction of nitroarenes, *RSC Adv.*, **2016**, 6, 31074-31082.
- [24] I. J. Turchi, The Chemistry of Heterocyclic Compounds, Oxazoles, Chapter 1, John Wiley & Sons Inc: USA, **1986**, 272.
- [25] G. Crank, M. Heville, R. Ryden, Thiourea Derivatives of 2-Aminooxazoles Showing Antibacterial and Antifungal Activity, *J. Med. Chem.*, **1973**, 16, 1402-1405.
- [26] M. Pattanayak, P.L. Nayak, Ecofriendly green synthesis of iron nanoparticles from various plants and spices extract, *Inter J Plant Animal & Environ. Sci*, **2013**, 3, 68-78.
- [27] V. Singh, S. Tiwari, S. Pandey, Preeti, R. Sanghi, Cassia grandis seed gum-graft-poly(acrylamide)-Silica hybrid: An excellent cadmium(II) adsorbent, *Adv Mater Lett*, **2015**, 6, 19-26.
- [28] D. C. Gowda, B. Neelisidaiah, Y. V. Anjaneyalu, Structural studies of polysaccharides from aloe vera, *Carbohydr. Res.*, **1979**, 72, 201-205.
- [29] H. Chen, Y. Cao, E. Wei, T. Gong, X. Quiming, Facile synthesis of graphene nano zero-valent iron composites and their efficient removal of trichloronitromethane from drinking water, *Chemosphere*, **2016**, 146, 32-39.
- [30] R. Stolle, P.E. Bowles, UberThiocarbohdrazid, *Chem. Ber.*, **1908**, 41, 1099-1102.
- [31] L. Ruangpan, E. A. Tendencia, Laboratory manual of standardized methods for antimicrobial sensitivity tests for bacteria isolated from aquatic animals and environment, Chapter 2, Aquaculture Department, Southeast Asian Fisheries Development Center. **2004**, 14-29.
- [32] Z. N. Siddiqui, F. Farooq, T.N. Mohammad Mustafa, A. Ahmad, A.U. Khan, Synthesis, characterization and antimicrobial evaluation of novel halopyrazole derivatives, *J. Saudi Chem. Soc.*, **2013**, 17, 237-243.

#### AUTHORS' ADDRESSES

1. **Jadveer Singh**

Department of Chemistry, University of Allahabad, Allahabad-211002  
E-Mail: jadveer007@gmail.com

2. **Dr. Preeti**

Department of Chemistry, University of Allahabad, Allahabad-211002  
E-Mail: preetisrivastava.au@gmail.com

3. **Arvind Kumar Pandey**

Department of Chemistry, University of Allahabad, Allahabad-211002  
E-Mail: arvindauchem@gmail.com

4. **Sneha Joshi**

Department of Chemistry, University of Allahabad, Allahabad-211002  
E-Mail: snehajoshi008@gmail.com

5. **Lalit Mohan Dwivedi**

Department of Chemistry, University of Allahabad, Allahabad-211002  
E-Mail: dwivedilalitmohan@gmail.com

6. **Nauseen Fatima**

Department of Chemistry, University of Allahabad, Allahabad-211002  
E-Mail: nfnrau786@gmail.com

7. **Dr. Shailendra Tiwari**

Department of Chemistry, University of Allahabad, Allahabad-211002

E-Mail: drshailendratiwariau@gmail.com

8. **Prof. Vandana Singh**

Department of Chemistry, University of Allahabad, Allahabad-211002

E-Mail: vschemau@gmail.com